Damage Detection Using Measurement Response Data of Beam Structure Subject to a Moving Mass

Abstract

The moving load problem is divided into two typical types: moving force and moving mass. The moving mass problem includes the time-varying mass effect. This work considers damage detection of the beam structure subject to a moving load including the inertia effect based on the only measurement data from strain gages and accelerometers without any baseline data. This experiment compares the feasibility of damage detection methods depending on the measurement sensors of strain gages and accelerometers. The measurement data are transformed to the proper orthogonal modes (POMs) in the time domain and the frequency domain, respectively. The magnitude of the moving mass and its velocity are also evaluated as test variables in this experiment. It is shown in the beam tests that the measured strain data can be more explicitly utilized in detecting damage than the acceleration data, and the mass magnitude and its velocity affect the feasibility of damage detection.

Keywords

damage detection, moving mass, proper orthogonal mode, inertia effect, strain gage, accelerometer.

Eun-Taik Lee [a]
Hee-Chang Eun [b]

[a] Department of Architectural Engineering, Chung-Ang University, Seoul, Korea, etlee@cau.ac.kr

[b] Department of Architectural Engineering, Kangwon National University, Chuncheon, Korea, heechang@kangwon.ac.kr

1 INTRODUCTION

The dynamic response of the beam structure traversed by moving systems has been studied during the last several years. The moving load problem is divided into two typical types, namely moving force and moving mass, depending on the inertia interaction of the moving mass and its supporting member. Neglecting the inertia interaction of the moving load and its supporting structure, the external load acts as the moving force. The moving force problem assumes the magnitude of the moving force is constant because the inertia effect is neglected. Considering the inertia interaction of the mass and beam leads to a moving load in the form of moving mass.

A time-varying (non-stationary) system due to the inertia effect leads to the change of the modal parameters at each time instant. The velocity of the moving mass and the ratio of the moving mass to that of the supporting structure affect the dynamic responses of the supporting member.

There have been many attempts to analytically solve moving load problems such as moving mass and moving sprung mass problems. Pesterev *et al.* (2003) investigated the asymptotic behavior of the solution for the moving oscillator problem. They discussed that in case of infinite spring stiffness, the moving oscillator problem leads to the moving mass problem. For small spring stiffness, it is equivalent to the moving force problem. Azam *et al.* (2013) evaluated the dynamic responses of a Timoshenko beam subjected to a moving mass and a moving sprung mass using Hamilton's principle. Mao and Lu (2013) developed a resonance severity indicator for an assessment of the resonance effect involving moving loads and moving masses. Dehestani *et al.* (2009) presented an analytical-numerical method to determine the dynamic response of beams carrying a moving mass with various boundary conditions and investigated critical influential speeds in the moving mass problems. Yavari *et al.* (2002) investigated the effects of beam thickness and moving mass velocity on the dynamic response of Timoshenko beams under moving mass using the discrete element technique. Garibaldi *et al.* (2011) established the connection among the natural frequency, signal amplitude and nonlinearity to eliminate the nonlinear contribution. The method can estimate the carriage characteristics such as mass and velocity.

The derived dynamic responses of the beam structure subject to a moving mass have been applied to its damage detection. Bilello and Bergman (2004) provided an analytical tool for the analysis of a damaged beam under a moving mass. Bellino *et al.* (2009) presented a time-varying identification method to detect a crack in a beam with a moving mass. Considering that natural frequencies of real structures are affected by environmental conditions such as the mass and the velocity of the train, Bellino *et al.* (2010) established the relationship between the natural frequencies and the load characteristics. They proposed a damage identification method to detect the presence of damage in a railway bridge crossed by a train using the principal component analysis. Wahab and De Roeck (1999) investigated the application of the change in modal curvatures to detect damage in a prestressed concrete bridge. Zhu and Hao (2007) developed a method to detect the damage in a bridge beam structure under load environments modeled by a group of vehicle-bridge interaction forces moving at a prescribed velocity. Pala and Reis (2013) studied the effects of inertial, centripetal, and Coriolis forces on the dynamic response of a simply supported beam with a single crack under moving mass load. Analyzing the time response of a cracked beam carrying moving mass and combining continuous and discrete wavelet transforms, Gokdag (2011) proposed a damage detection method. This research mentions that strain data outperform displacement data at the same point in revealing the damage signature. Cavadas *et al.* (2013) presented a damage detection approach for using moving-load responses as time series based on two data-driven methods of moving principal component analysis and robust regression analysis. Using the generalized multi-symplectic formulations, Hu *et al.* (2013) considered the dynamic behavior of continuous beams under moving load. Nikkhoo *et al.* (2014) studied the vibration of a rectangular plate due to multiple traveling masses.

Most of the damage detection methods require knowledge of fundamental information for a structure without damage, and they are not very suitable for practical structures where baseline data cannot be readily obtained. The structural performance should be evaluated by only measured data at the damaged state. An accelerometer as a measurement sensor can be intermittently attached and measured if necessary, but a strain gage is retained for measurement until it is removed after installation. The strain gage is pertinent to the long-term measurement and the accelerometer to the short-term measurement. The contaminated response sets containing external noise are utilized as the basic information for detecting damage. The damage is detected by investigating the responses by using the noise. The proper orthogonal decomposition (POD) extracts features by revealing a relevant, but unexpected, structure hidden in the data. The POD is used to derive a reduced-order model for non-linear initial value problems.

This work investigates damage detection of a beam structure subject to a moving load including the inertia effect based on only measurement data from strain gages and accelerometers without any baseline data. The feasibility of damage detection by using accelerometers and strain gages is compared. The measurement data are transformed to proper orthogonal mode (POM) to reduce the inertia and noise effects and to investigate the damage present. The magnitude of the moving mass, its velocity and the types of measurement sensors are utilized as the test variables in this experiment. It is shown in the beam tests that the measured strain data can be more explicitly utilized in detecting damage than the acceleration data, and the mass magnitude and its velocity affect the applicability of damage detection.

2 DYNAMIC RESPONSE OF A BEAM STRUCTURE SUBJECT TO A MOVING MASS

The moving mass analysis should be considered to predict the dynamic responses of a beam structure subject to a moving mass. The dynamic response of the beam in Figure 1 is affected by the traveling velocity of the moving mass and its magnitude. The moving mass problem assumes that the stiffness of the moving system is infinite and neglects the possibility that the mass may separate from the beam. Based on energy methods, the equation of motion for an Euler-Bernoulli beam of length L travelled by a mass M with velocity $v(t)$ is expressed by
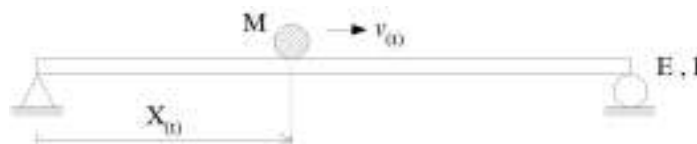
Figure 1: A beam structure subject to a moving mass.

$$EI\frac{\partial^4 y}{\partial x^4}(x,t) + m\frac{\partial^2 y}{\partial t^2}(x,t) = -M\left[g + v^2\frac{\partial^2 y}{\partial x^2} + 2v\frac{\partial^2 y}{\partial x \partial t} + \frac{\partial^2 y}{\partial t^2}\right]\delta(x - \hat{x}(t)) \tag{1}$$

where $y(x,t)$ is the vertical deflection of the beam; m and I are the mass per a unit length and the area moment of inertia, respectively; $\hat{x}(t) = vt$ is the instantaneous position of the mass along the beam; $\delta(x)$ is the Dirac delta function and g is the acceleration of gravity. It is shown in Eq.

(1) that the dynamic responses of the beam are affected by the velocity of the moving mass and the ratio of the moving mass to that of the supporting structure. Taking them as the test variables, this study performs the experiments using the measurement sensors of strain gages and accelerometers to evaluate the feasibility of damage detection.

3   EXPERIMENTAL STUDY

The applicability of damage detection on a simply supported beam is examined depending on the test variables and measurement sensors. A steel beam in Figure 2 is 1200mm in length, and its gross cross-section is $100\text{mm} \times 11\text{mm}$. The damage is located at 350mm between nodes 3 and 4 from the left end, and its cross-section is $110\text{mm} \times 8\text{mm}$. The response data in the time domain are sequentially measured by 11 strain gages and accelerometers installed in advance at the bottom of the beam without the action of any external force. The damage is traced by the measurement data only and without any baseline data. Both experiments using strain gages and accelerometers are conducted using DYTRAN model 3055B1 uniaxial accelerometers and TML strain gages of type FLA-5-11, respectively. The data in the time domain are collected by a DEWE-TRON model DEWE-43.
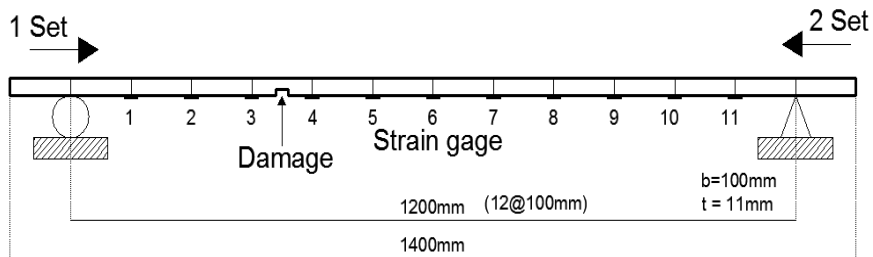
Figure 2: A simply supported beam structure subject to a moving mass.

Figure 3: A battery-operated toy car and magnet mass.

(a)

(b)

(c)

(d)

(e)

(f)
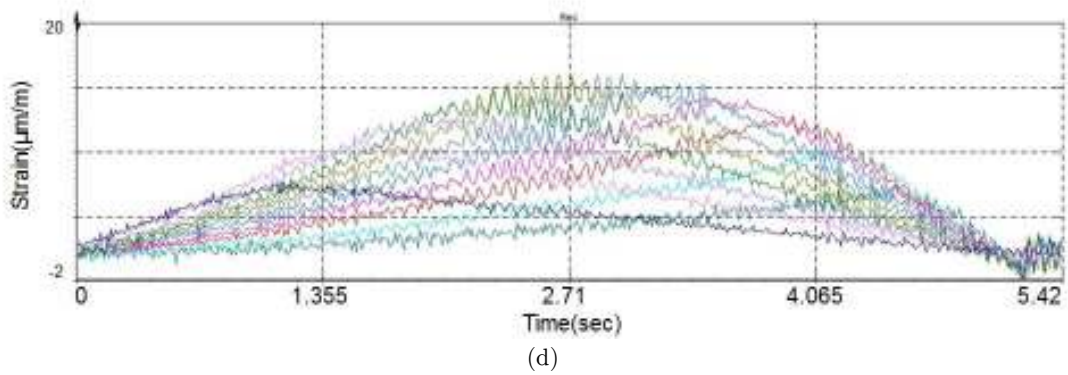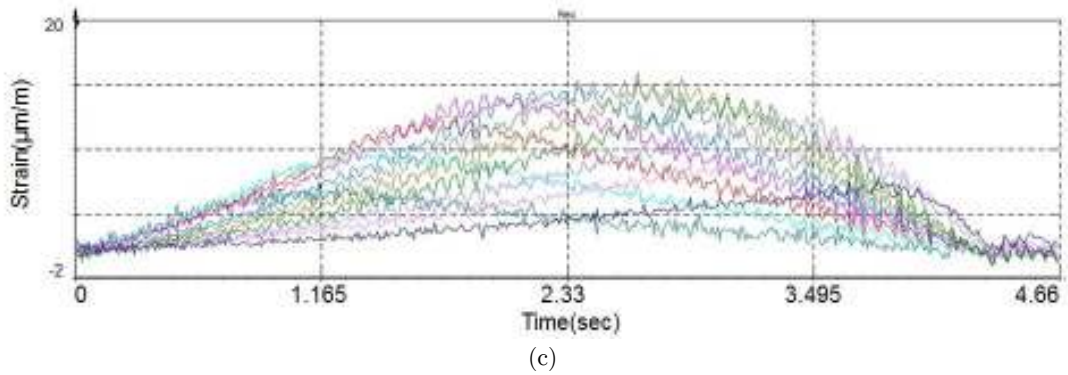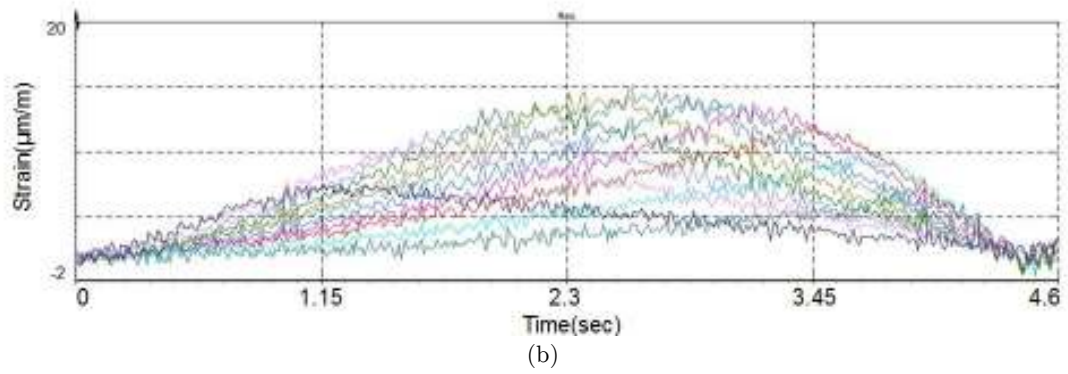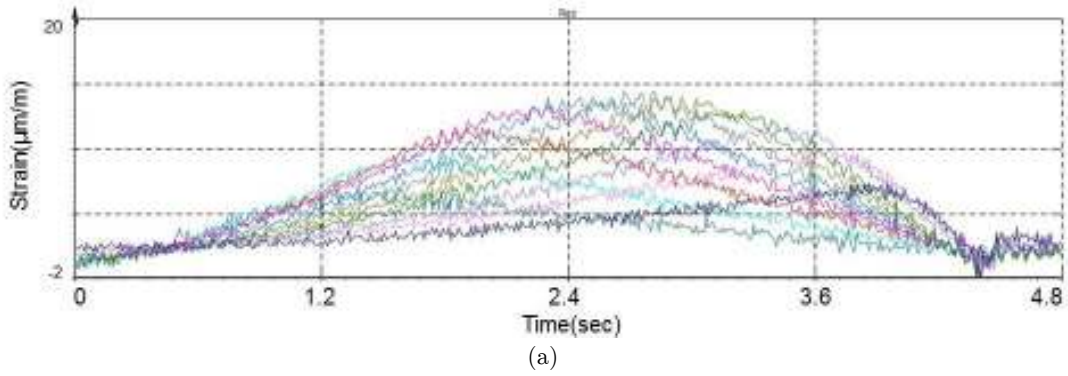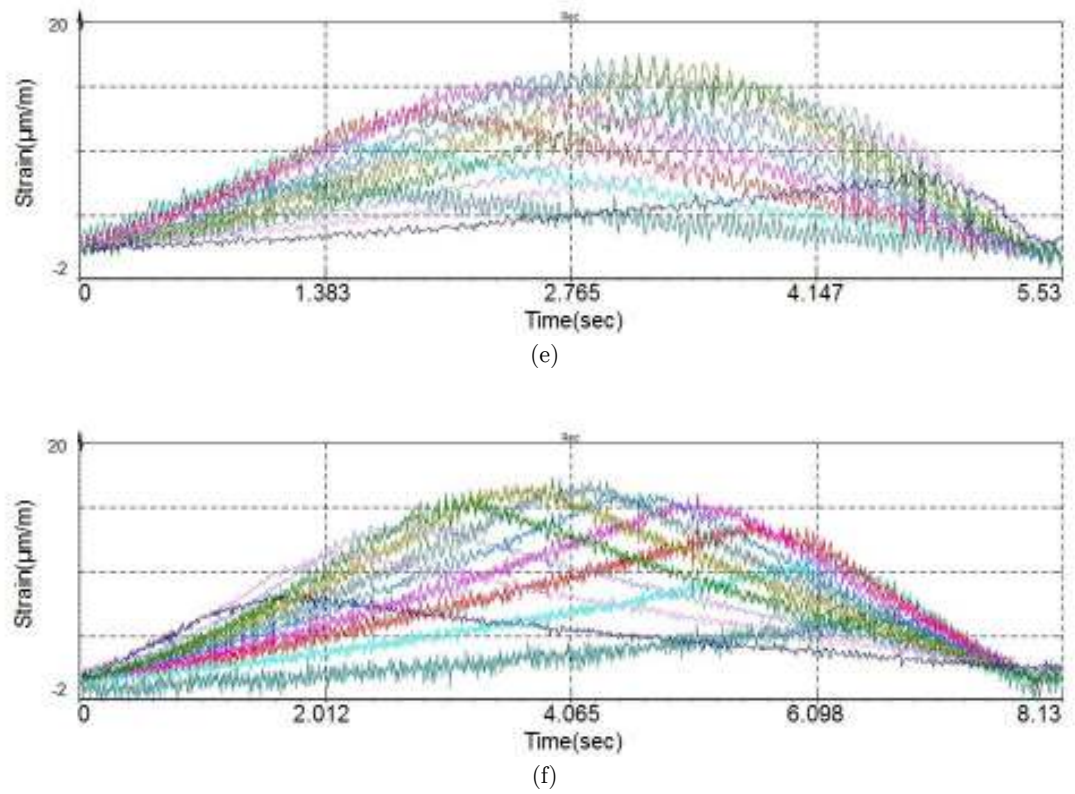
Figure 4: Strain response in the time domain: (a) 2.3-R, (b) 2.3-L. (c) 2.5-R, (d) 2.5-L, (e) 2.74-R, (f) 2.74-L.

(a)

(b)
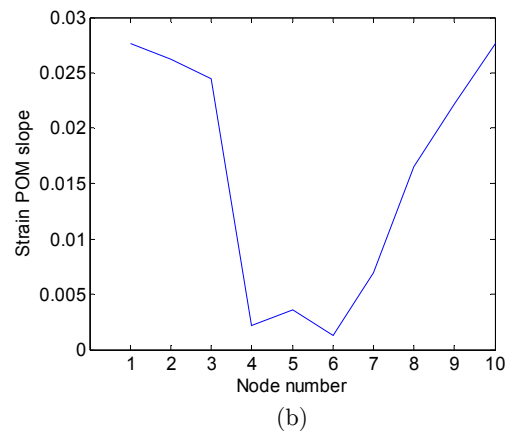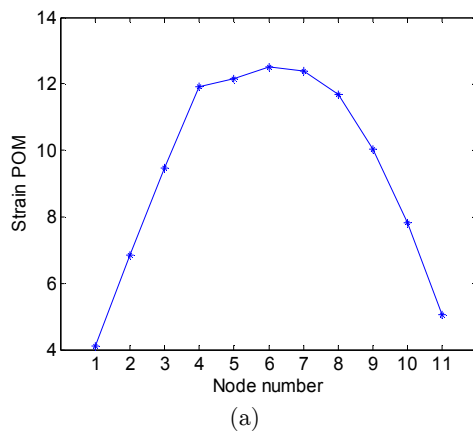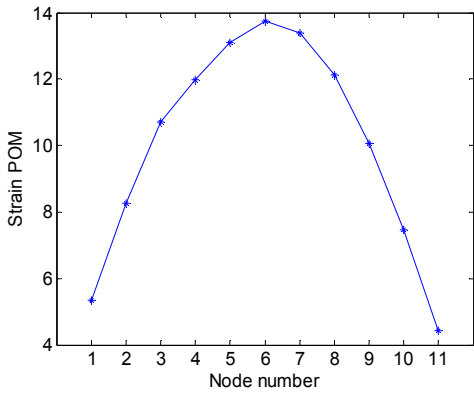
(c)
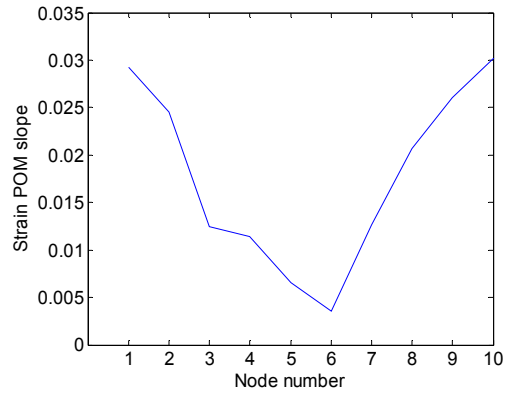
(d)
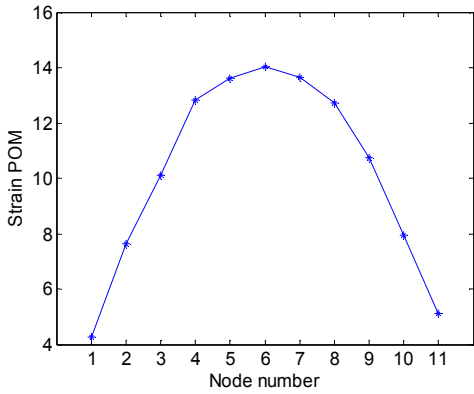
(e)
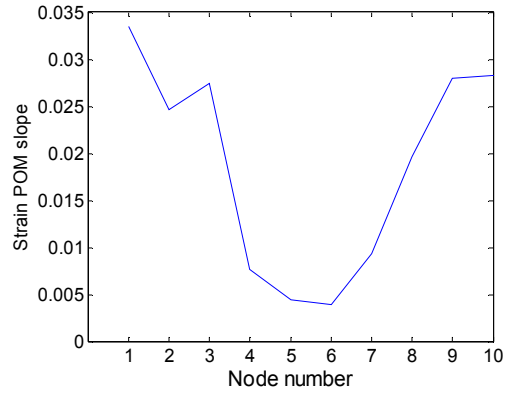
(f)
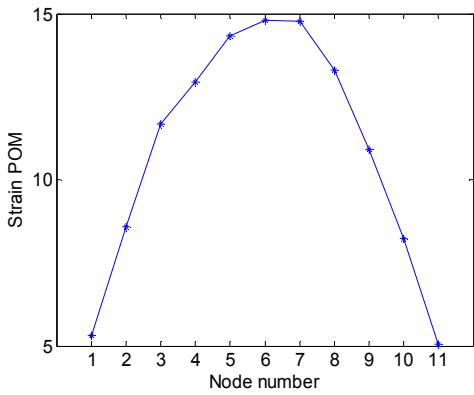
(g)
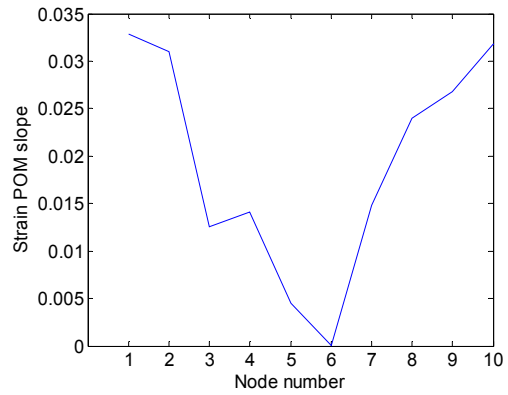
(h)
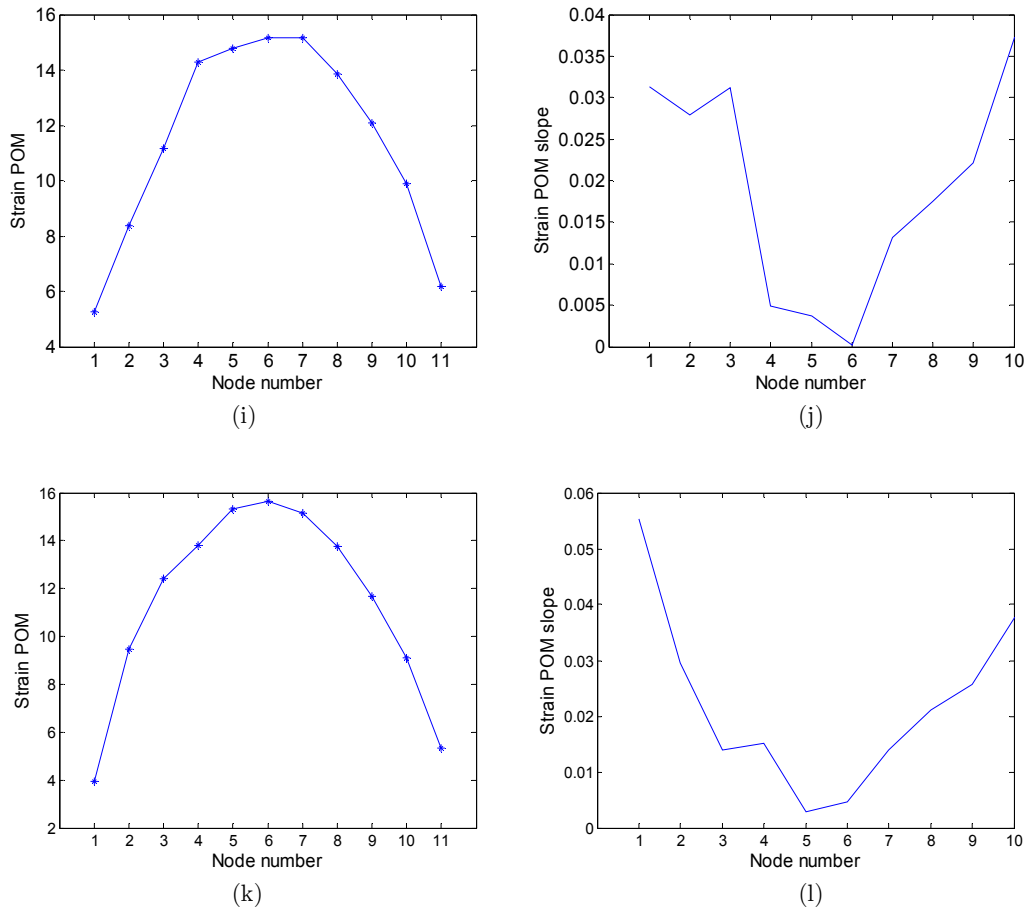
Figure 5: Strain POM and its slope along the beam member: (a) 2.3-R, (b) 2.3-R,
(c) 2.3-L , (d) 2.3-L, (e) 2.5-R, (f) 2.5-R, (g) 2.5-L, (h) 2.5-L, (i) 2.74-R,
(j) 2.74-R, (k) 2.74-L, (l) 2.74-L

A battery-operated toy car functions as the moving mass by using a sum of the self-weight of the car and the weight of steel magnets. It is shown in Figure 3 that the stiffness of the toy car is very high. The moving velocity and the time required from an end support to the other end support decreases with an increase in the moving mass. Accelerating gradually from rest, the moving mass does not travel at a constant velocity, and the system is considered a time-varying system. This study utilized the average velocity expressed by the distance covered with respect to the time taken. The mass magnitude is not inversely proportional to its velocity. A response dataset is collected by the moving mass in a rightward direction and another dataset in a leftward direction.

The total weight of the steel beam as the supporting member is 13kg . The moving masses, including the weight of steel magnets and the self-weight of the car, are 2.3kg , 2.5kg and 2.74kg .

Experimental data are collected from two different types of measurement sensors of strain gages and accelerometers, and the feasibility of the measurement sensors for damage detection are compared. For the first test, the damage detection of the steel beam is performed using the measurement data from the strain gages. The strain gages are bonded in the interval of 100mm on the bottom of the beam section. Two datasets in the rightward and leftward directions according to the movement directions of the car are simultaneously collected by 11 strain gages as shown in Figure 2. The moving mass and its average velocity obtained in the experiment are displayed in Table 1. Figure 4 represents the strain responses in the time domain as each mass of 2.3kg, 2.5kg and 2.74kg moves an end support to the other end support. In the plots, R and L denote the rightward and leftward directions, respectively. It is observed that the plots do not exhibit the information on the damage because of the external noise included in the measured data. Most noise comes from the vibration of the motor in the car. To minimize the noise effect included in each strain dataset, the POM corresponding to the first proper orthogonal value (POV) is extracted from three strain datasets within the time that the moving mass arrives at the same position as the strain gage. The POMs of strains at all nodes are displayed in Figure 5. The plots show that it is not easy to explicitly find the damage location based on the strain curves regardless of the inertia effect. Considering that the variation in the slope of the strain curves is sensed, the slope curves of the strains are described in Figure 5. The slope indicates the variation of the strain along the nodes. It is found that the damage is located at the nodes to exhibit the abrupt variation of strains as shown in three different cases. The plots also show that the damage can be more explicitly detected as the moving mass increases or the average moving velocity decreases.

Moving mass	2.3kg	2.5kg	2.74kg
Moving mass ratio (%)	17.7	19.2	21.1
Average velocity of the car	337.8mm/sec.	304.9mm/sec.	240.4mm/sec.
	320.5mm/sec.	261.8mm/sec.	172.7mm/sec.

Table 1: Test variables of mass magnitude and its velocity.

Another beam test for damage detection was performed by the measurement of accelerometers as shown in Figure 6. The acceleration responses in the time domain are measured at 11 nodal positions and are represented in Figure 7. It is shown that the acceleration responses, including external noise in the time domain, do not provide any information on the damage. The acceleration response in the time domain is transformed to the FFT in the frequency domain. Figure 8 represents the magnitude of the responses in the frequency domain. Neglecting a slight difference in the first resonance frequency due to the inertia effect, three FFT datasets in the neighborhood of the first resonance frequency are selected because it is not easy to collect the exact data at the first resonance frequency moment. In addition, the datasets are transformed to the POM. Figure 9 represents the POM curves. It is observed that they do not have consistent shapes depending on the mass magnitude so that the damage cannot be recognized at the same location. The measurement data from accelerometers are more sensitive to the external noise and the mass magni-

tude than from the strain gages. The beam structure is characterized by the flexural behavior such as the curvature. Based on the flexural characteristics, the abrupt variation of the curvature should be located near the damage region.

This study utilizes the POM curvature to evaluate the damage of the beam. The POM curvature corresponding to the l-th $(l = 1,2,...,n)$ POM at each location k on the structure can be numerically obtained using a central difference approximation:

$$C_{kl} = \frac{D_{(k-1)l} - 2D_{kl} + D_{(k+1)l}}{h^2}, \quad k = 2,3,\cdots,n-1 \tag{2}$$

where C_{kl} is the second derivatives of the kth flexural dimension, l denotes the corresponding POV, and h is the distance between two successive nodes. Figure 9 represents the POM curvature curves. The plots on the POM and its curvature corresponding to the mass magnitudes of 2.3kg, and 2.5kg in Figures 9(a) through (d) and (e) through (h) do not provide information on the damage, respectively, but the plots of 2.74kg in Figures 9(i) through (l) do. In the case of the mass of 2.74kg, the curvature curve taken from the mass and the beam moving in the leftward direction provide more accurate information than the rightward direction. This indicates that it is not easy to detect damage during the acceleration process from rest. From the experiments, the measurement from strain gages provides more conservative damage information than the accelerometers. In addition, the accelerometers are sensitively affected by the mass magnitude of the car unlike the strain gages.
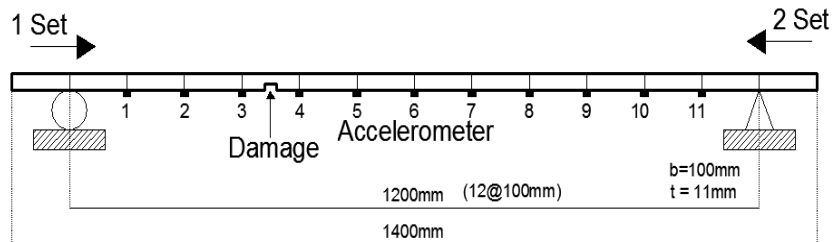
Figure 6: A simply supported beam subject to a moving mass (accelerometer sensors).
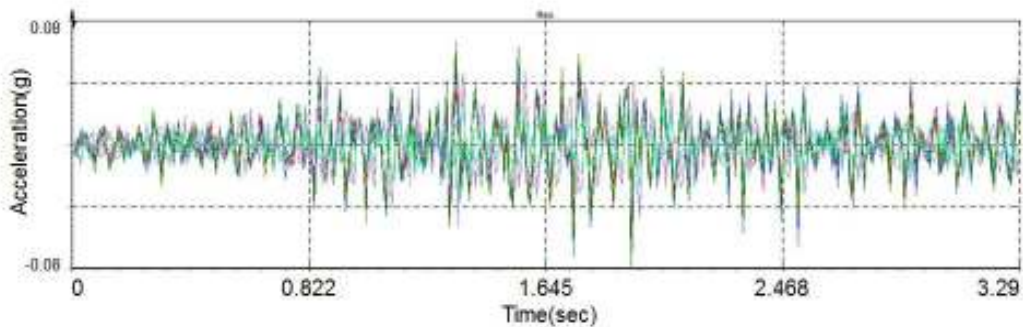
(a)
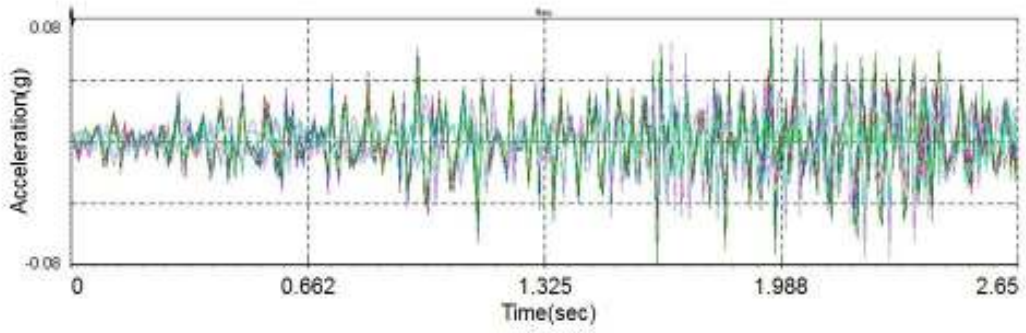
(b)
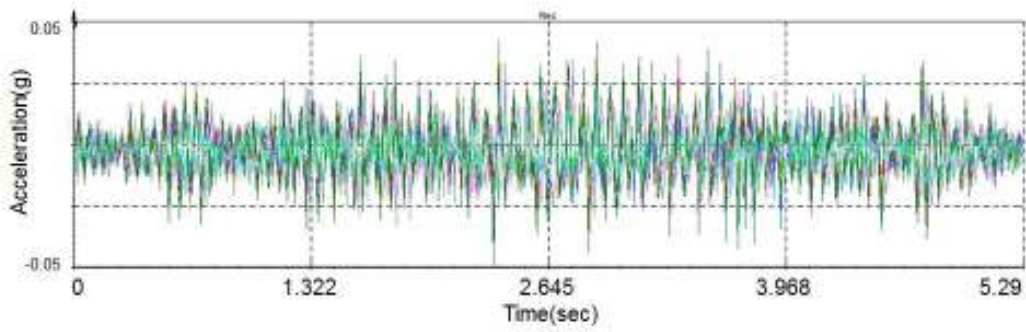
(c)
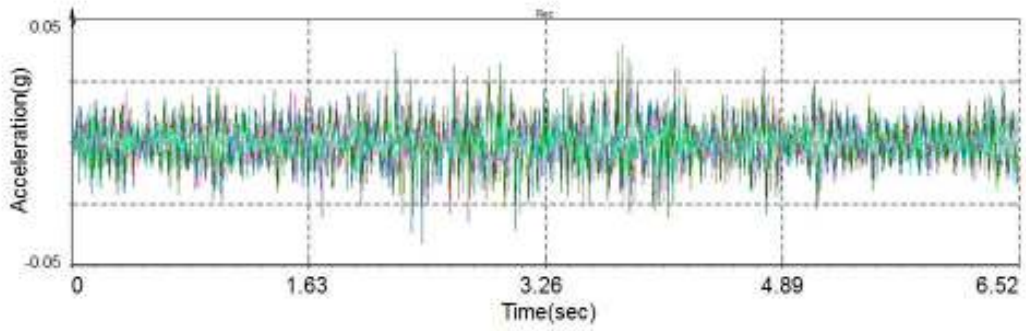
(d)
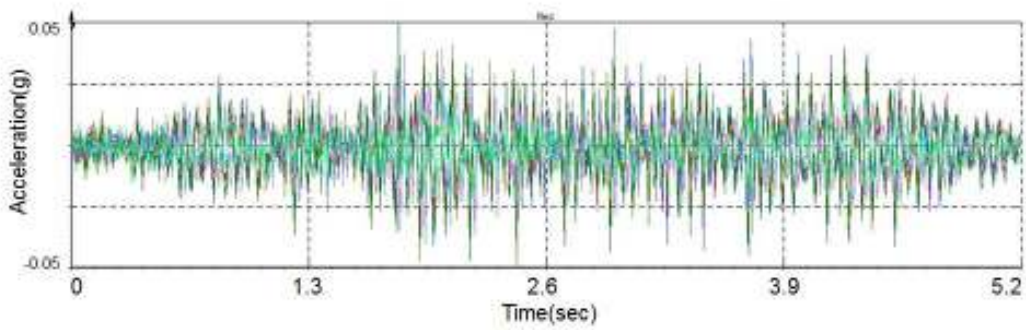
(e)
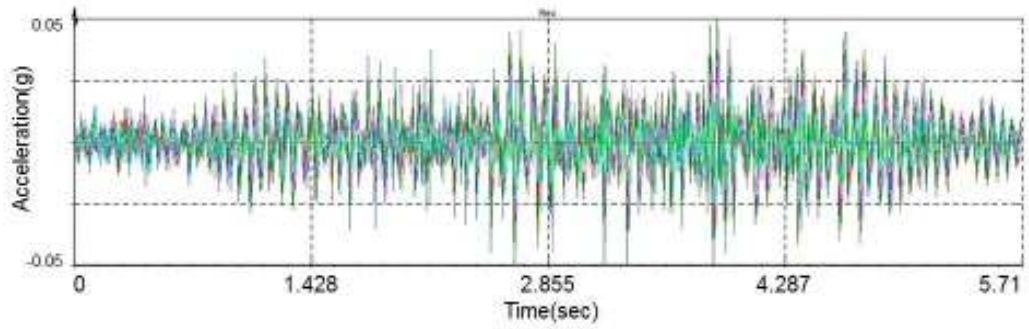
(f)

Figure 7: Acceleration responses in the time domain:
(a) 2.3-R, (b) 2.3-L, (c) 2.5-R, (d) 2.5-L, (e) 2.74-R, (f) 2.74-L.

(a)

(b)

(c)

(d)

(e)

(f)
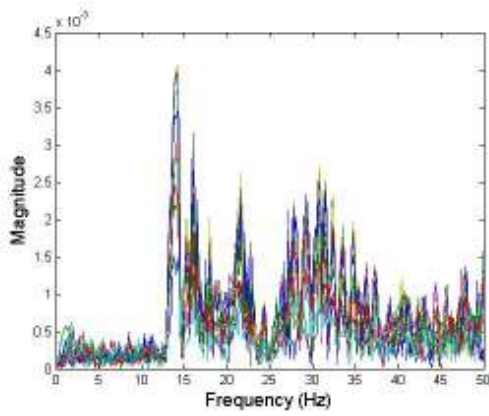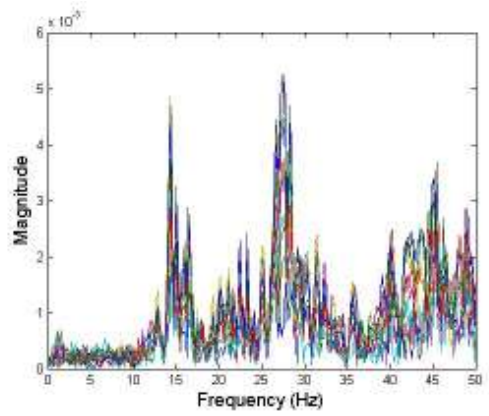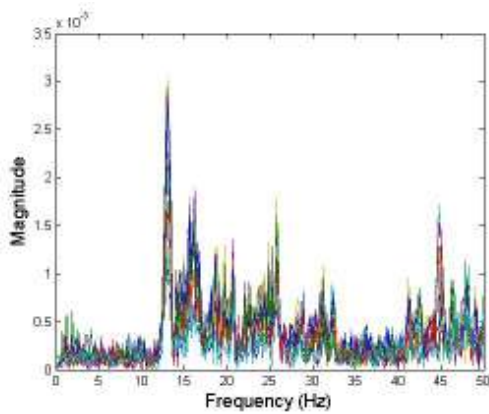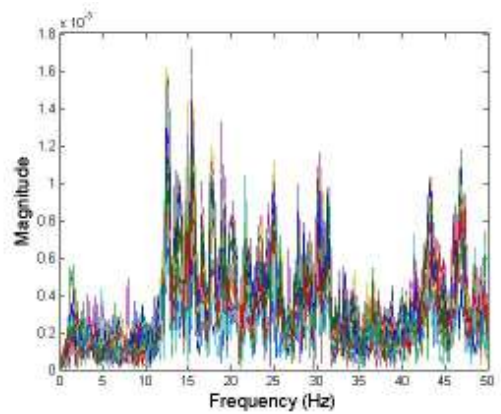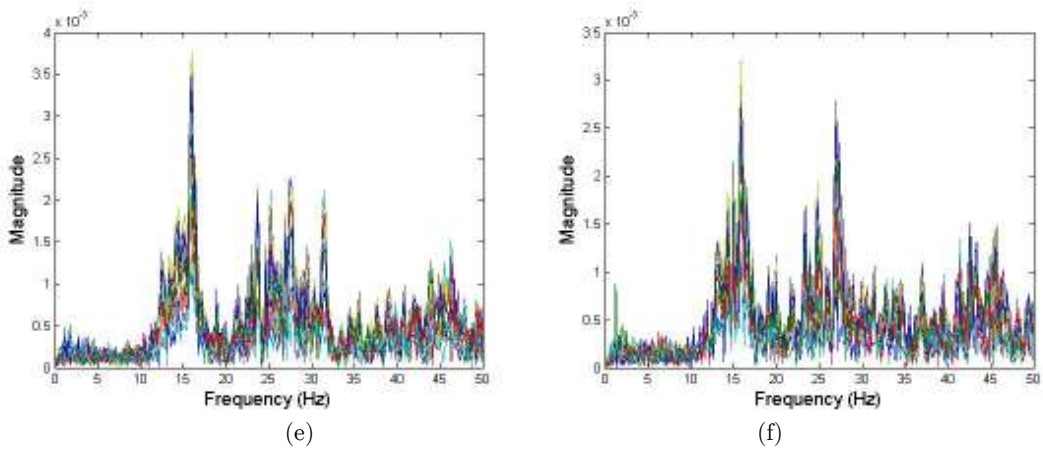
Figure 8: FFT transform: (a) 2.3-R, (b) 2.3-L, (c) 2.5-R, (d) 2.5-L, (e) 2.74-R, (f) 2.74-L.

(a)

(b)

(c)

(d)
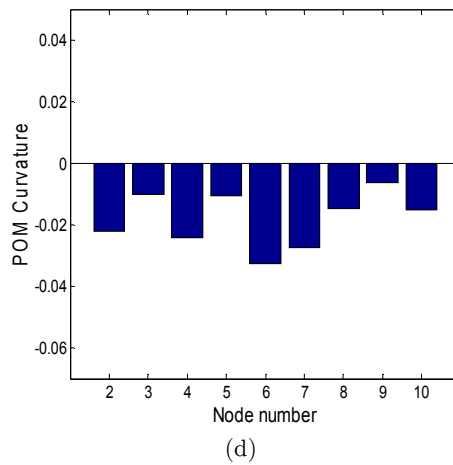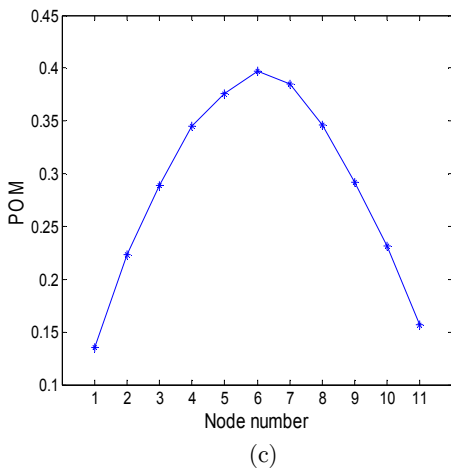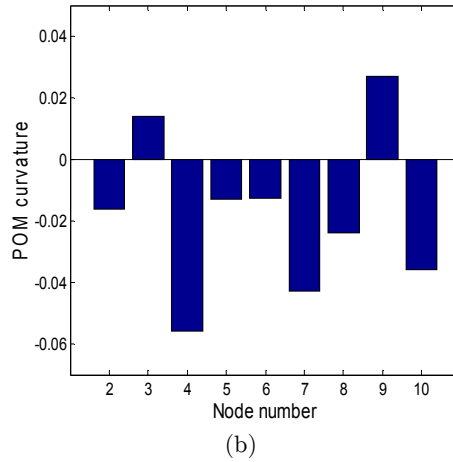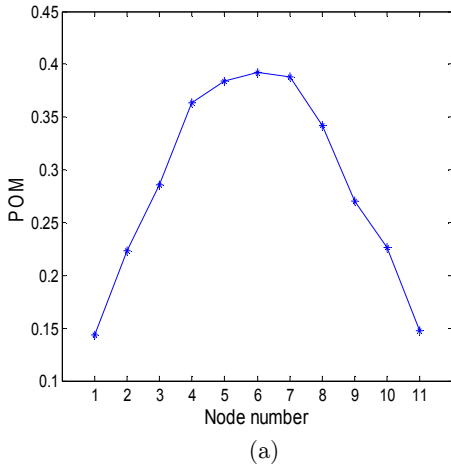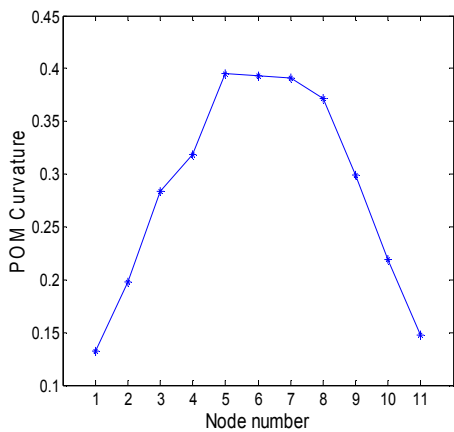
(e)
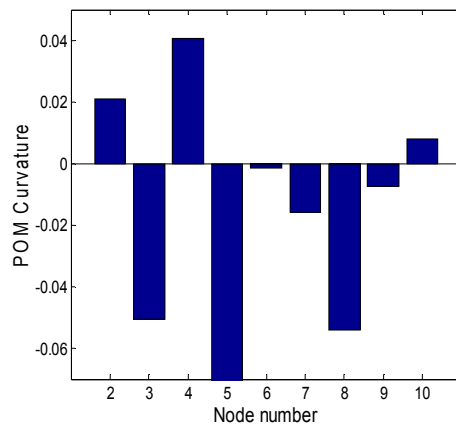
(f)
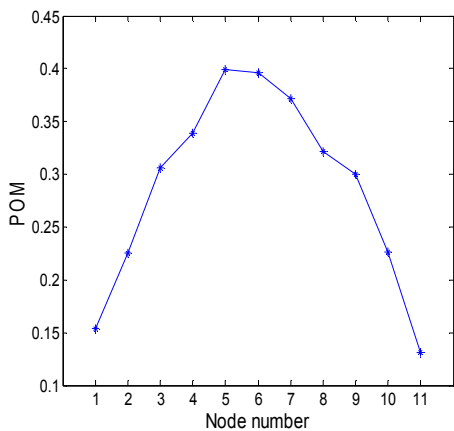
(g)
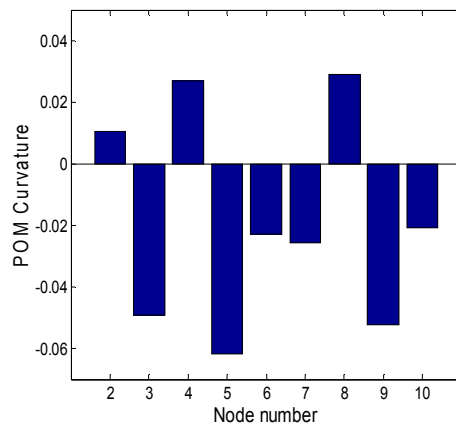
(h)
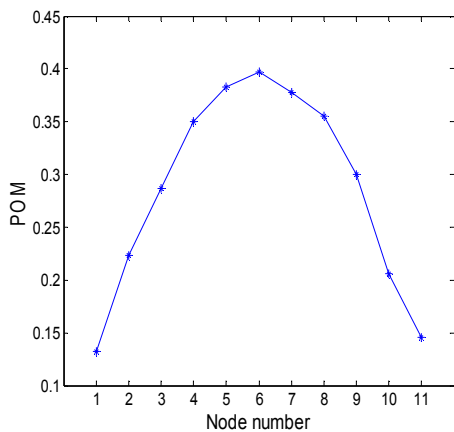
(i)
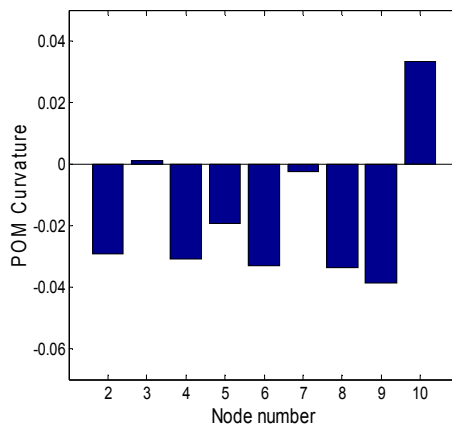
(j)
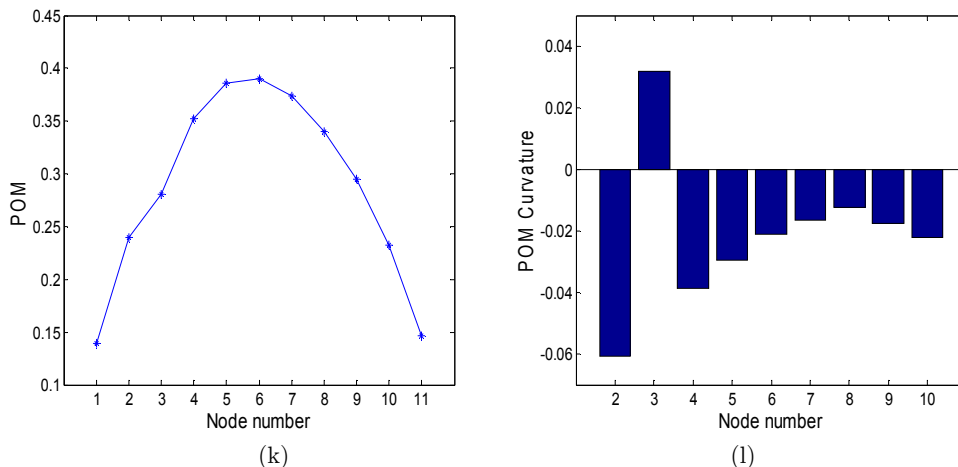
Figure 9: POM and its curvature: (a) 2.3-R, (b) 2.3-R,
(c) 2.3-L , (d) 2.3-L, (e) 2.5-R, (f) 2.5-R, (g) 2.5-L, (h) 2.5-L, (i) 2.74-R,
(j) 2.74-R, (k) 2.74-L, (l) 2.74-L.

The applicability of the damage detection method at beam structure considering subject to a moving mass is investigated by a numerical experiment. The test beam in Figure 2 is also utilized as the analytical model. A beam with a length of 1.2 m was modeled using 12 beam elements. The beam has an elastic modulus of $2.0 \times 10^5 \, \text{MPa}$ and a unit mass of 7,860 kg/m^3. The beam's gross cross section is $100\text{mm} \times 10\text{mm}$ and its damage section is established as the reduction of 30% flexural rigidity at element 4. The damping matrix is assumed as a Rayleigh damping to be expressed by the stiffness matrix and a proportional constant of 0.0001. The mass of 2.3kg is assumed to travel with a velocity of 337.8mm/sec. This work neglects the external noise and the analysis is carried out following the procedure in Figure 10.

The dynamic responses of the beam are obtained by solving the second order differential equation. The displacement responses at all nodes are displayed in Figure 11(a). It is shown that the dynamic transverse responses in the time domain do not provide the explicit information on the damage. Summing the absolute values of all displacements in the time span
$\begin{bmatrix} t0 & tf \end{bmatrix} = \begin{bmatrix} 0 & 3.5524 \, \text{sec.} \end{bmatrix}$ where $t0$ and tf represent the beginning and final time to be integrated, respectively, the responses are normalized as follows:

$$\widetilde{y}_i = \frac{\left| \sum_l y_{il} \right|}{\left\| \sum_l y_{il} \right\|} , \quad l = 1, 2, ..., r \tag{3}$$

Where $\widetilde{y}_i$ denotes the normalized displacement of summed-absolute displacements at node i and l is the number of time step to be integrated. And $|\bullet|$ is the absolute and $\|\bullet\|$ is the norm. Figure 11(b) and 11(c) represent the normalized displacement and its curvature. The curvature is estimated by a central difference method. Both plots also do not indicate explicit damage. Conside-

ring the curvature is proportional to the flexural strain, Figure 11(d) displays the slope of the curvature related to the flexural strain. It is observed that the slope between two adjacent nodes 4 and 5 in the neighborhood of the damage is abruptly changed. It is expected that the damage can be detected by analyzing the displacements of the beam subject to a moving mass.

The 300 displacement response data sets between 1.2569 sec. and 1.4197 sec. are extracted to transform to the POM. Figure 11(e) and 11(f) display the POM corresponding to the first POV. It is observed that the POM curvature is abruptly changed between two nodes 4 and 5. From this numerical experiment, the validity of the proposed method to detect damage based on the flexural responses of beam structure due to the moving mass is verified.
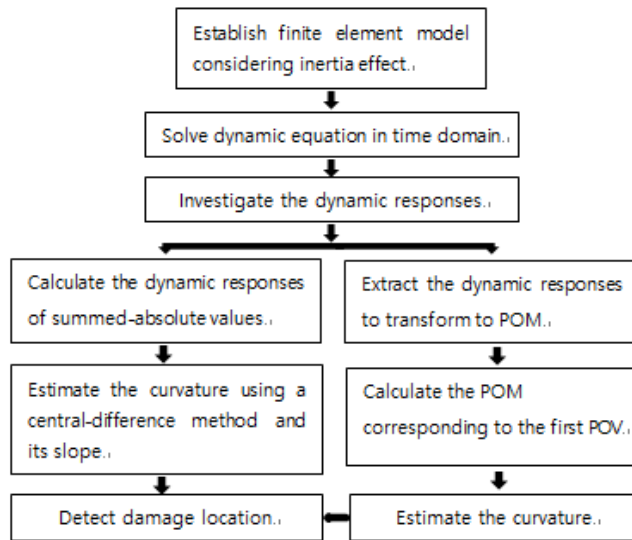
Figure 10: Flow chart for finite element analysis.

(a)

(b)
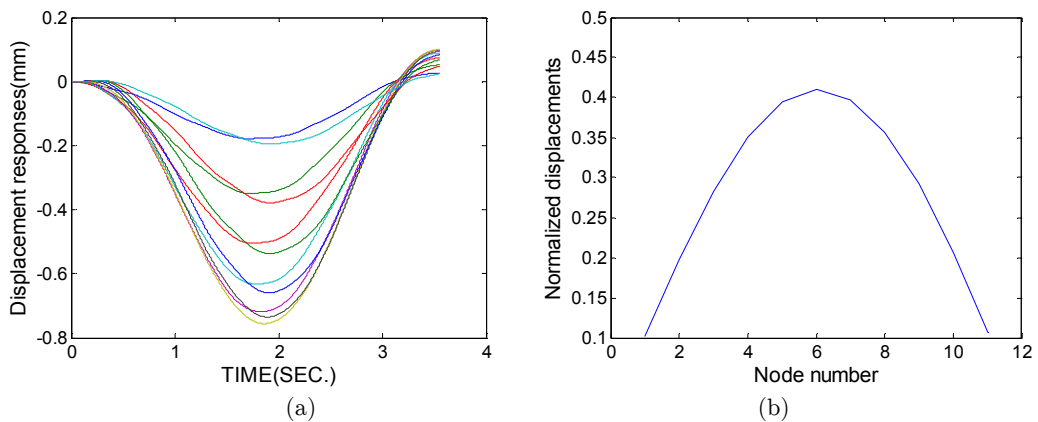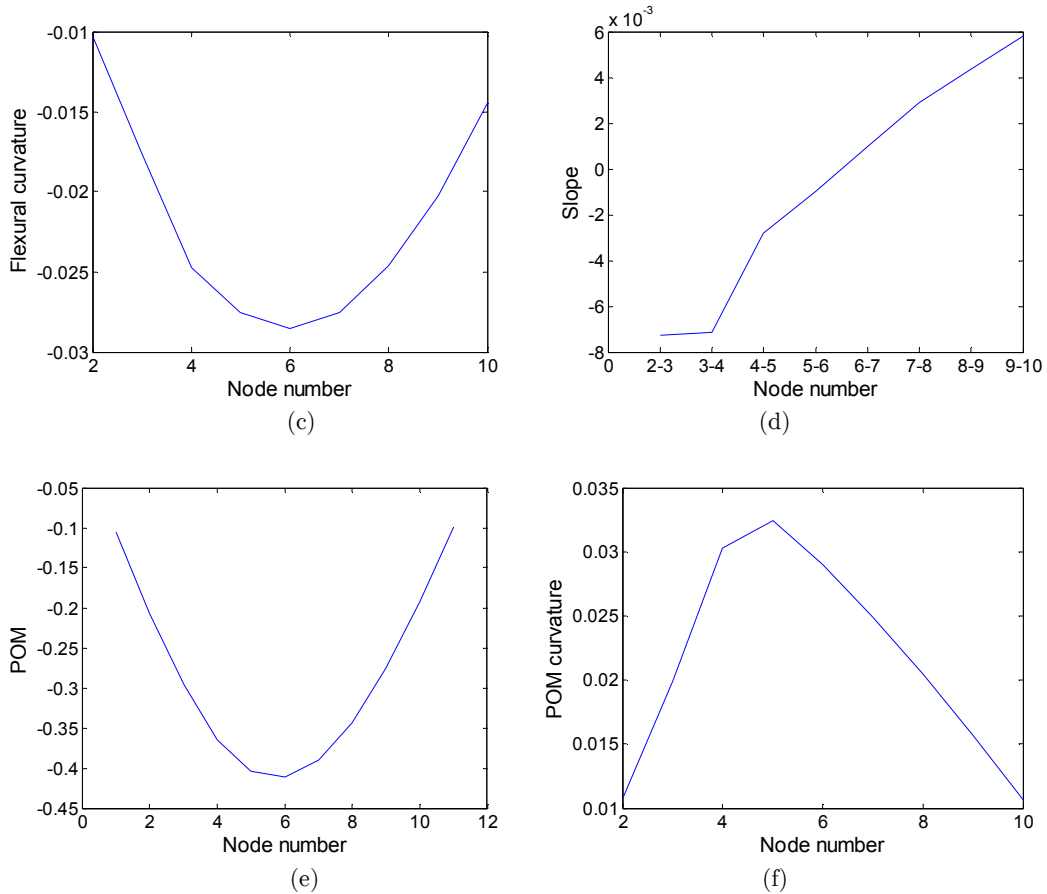
Figure 11: Numerical results: (a) displacement responses, (b) normalized responses
of summed-absolute displacements, (c) flexural curvature, (d) slope of curvature,
(e) POM corresponding to the first POV, (f) slope of the POM.

4   CONCLUSIONS

This work investigated the feasibility of damage detection of a damaged beam structure subject
to a moving mass depending on the mass magnitude, its velocity and the measurement sensors.
The experimental results represent that the damage detection using strain gages provides more
accurate information on the damage than accelerometers. It is observed that the damage detec-
tion from strain gages can be taken more explicitly as the mass magnitude increases and its velo-
city decreases. The measurement data from accelerometers are more sensitive to the external noi-
se and the mass magnitude than strain gages. The experimental results show that it is not easy to
detect the damage when using accelerometers during the acceleration process from rest.

References

Azam, S.E., Mofid, M., Khoraskani, R.A., (2013). Dynamic response of Timoshenko beam under moving mass, Scientia Iranica A 20(1): 50-56.

Abu Husain N., Ouyang H., (2011), Detection of damage in welded structure using experimental modal data, Journal of Physics: Conference Series 305, doi:10.1088/1742-6596/305/1/012120.

Bellino, A., Garibaldi, L., Marchesiello, S., (2009). Time-varying output-only identification of a cracked beam, Key Engineering Materials 413-414: 643-650.

Bellino, A., Garibaldi, L., Fasana, A., Marchesiello, S., (2010). Damage detection in time-varying systems by means of the PCA method, Proceedings of ISMA: 783-794.

Bilello, C. and Bergman, L.A., (2004). Vibration of damaged beams under a moving mass: theory and experimental validation, Journal of Sound and Vibration 274: 567-582.

Cavadas, F., Smith, L.F.C., Figueiras, J., (2013). Damage detection using data-driven methods applied to moving-load responses, Mechanical Systems and Signal Processing 39: 409-425.

Dehestani, M., Mofid, M., Vafai, A., (2009). Investigation of critical influential speed for moving mass problems on beams, Applied Mathematical Modelling 33: 3885-3895.

Garibaldi, L., Fasana, A., Marchesiello, S., Bellino, A., (2011). Time variant identification of damaged structures excited by moving loads, Proceedings of the 8th International Conference on Structural Dynamics, EURODYN 2011, Leuven, Belgium.

Gokdag, H., (2011). Wavelet-based damage detection method for a beam-type structure carrying moving mass, Structural Engineering and Mechanics 38(1): 81-97.

Mao, L. and Lu, Y. (2013). Critical speed and resonance criteria of railway bridge response to moving trains, Journal of Bridge Engineering-ASCE 18(2): 131-141.

Nikkhoo A., Hassanabadi M.E., Azam S.E., Amiri J.V., (2014), Vibration of a thin rectangular plate subjected to series of moving inertial loads, Mechanics Research Communications 55: 105-113.

Pesterev, A.V., Bergman, L.A., Tan, C.A., Tsao, T.C., Yang, B., (2003). On asymptotics of the solution of the moving oscillator problem, Journal of Sound and Vibration 260(3): 519-536.

Pala, Y. and M. Reis, M., (2013). Dynamic response of a cracked beam under a moving mass load, Journal of Engineering Mechanics 139(9): 1229-1238.

Wahab M.M.A. and De Roeck, G., (1999). Damage detection in bridges using modal curvatures: applications to a real damage scenario, Journal of Sound and Vibration 336: 217-235.

Yavari, A., Nouri, M., Mofid, M., (2002). Discrete element analysis of dynamic response of Timoshenko beams under moving mass, Advances in Engineering Software 33(3): 143-153.

Zhu, X.Q. and Hao, H., (2007). Damage detection of bridge beam structures under moving loads, IMAC-XXV: A Conference & Exposition on Structural Dynamics, Florida, USA.

Appendix

Assume that measurement data are expressed by a finite number of points in space and frequency. Expressing a set of FRF response data as $\hat{\mathbf{U}}$, suppose that m linear snapshots of the response $\hat{U}_i$ of size n are obtained by response measurements written as

$$\hat{\mathbf{U}} = \begin{bmatrix} \hat{\mathbf{U}}^{(1)} & \hat{\mathbf{U}}^{(2)} & \cdots & \hat{\mathbf{U}}^{(m)} \end{bmatrix} = \begin{bmatrix} \hat{U}_1^{(1)} & \hat{U}_1^{(2)} & \cdots & \hat{U}_1^{(m)} \\ \hat{U}_2^{(1)} & \hat{U}_2^{(2)} & \cdots & \hat{U}_2^{(m)} \\ \vdots & \vdots & \ddots & \vdots \\ \hat{U}_n^{(1)} & \hat{U}_n^{(2)} & \cdots & \hat{U}_n^{(m)} \end{bmatrix} \tag{A1}$$

where the superscript (j) represents the FRF data at the j-th frequency Ω_j, n denotes the number of measurement positions of the structure and m is the total number of frequency observations.

The POD of this discrete field involves solving the eigenvalue problem. Let $m \times m$ matrix $\widetilde{\mathbf{C}}$ be defined as

$$\widetilde{\mathbf{C}} = \hat{\mathbf{U}}^T \hat{\mathbf{U}} \tag{A2}$$

Solving the eigenvalue problem of Eq. (A2) at the core of the POD method, Eq. (A2) satisfies

$$\widetilde{\mathbf{C}} \boldsymbol{\varphi}_k = \lambda_k \boldsymbol{\varphi}_k, \quad k = 1, \cdots, m \tag{A3}$$

where the eigenvalues are arranged as follows:

$$\lambda_1 \geq \lambda_2 \geq \cdots \geq \lambda_m \geq 0 \tag{A4}$$

where the eigenvalues λ_k are the POVs and each eigenvector $\boldsymbol{\varphi}_k$ of the extreme value problem is associated with a POV λ_k. $\boldsymbol{\varphi}_1$ represents the eigenvector corresponding to the largest eigenvalue λ_1.

The POMs may be used as a basis for the decomposition of U. The POM associated with the greatest POV is the optimal vector. If the eigenvalues are normalized to unit magnitude, they represent the relative energy captured by the corresponding POM. The eigenvalue reflects the relative kinetic energy associated with the corresponding mode. The energy is defined as the sum of the POVs. The POMs are written as

$$\boldsymbol{\psi}^k = \frac{\sum_{i=1}^{m} \boldsymbol{\varphi}_i^k \hat{\mathbf{U}}^{(i)}}{\left\| \sum_{i=1}^{m} \boldsymbol{\varphi}_i^k \hat{\mathbf{U}}^{(i)} \right\|}, \quad k = 1, \cdots, m, \tag{A5}$$

The POMs are arranged as follows:

$$\boldsymbol{\psi} = \begin{bmatrix} \boldsymbol{\psi}^1 & \boldsymbol{\psi}^2 & \cdots & \boldsymbol{\psi}^m \end{bmatrix} \tag{A6}$$